Ni-based Heusler compounds: How to tune the magnetocrystalline anisotropy

H. C. Herper*
Department of Physics and Astronomy, Uppsala University, Box 516, 751 20 Uppsala, Sweden

(Received 25 January 2018; revised manuscript received 16 May 2018; published 9 July 2018)

Tailoring and controlling magnetic properties is an important factor for materials design. Here, we present a case study for Ni-based Heusler compounds of the type Ni_2YZ with Y = Mn, Fe, Co and Z = B, Al, Ga, In, Si, Ge, Sn based on first-principles electronic structure calculations. These compounds are interesting since the materials properties can be quite easily tuned by composition and many of them possess a noncubic ground state being a prerequisite for a finite magnetocrystalline anisotropy (MAE). We discuss systematically the influence of doping at the Y and Z sublattices as well as the effect of lattice deformation on the MAE. We show that in case of Ni_2CoZ the phase stability and the MAE can be improved using quaternary systems with elements from main group III and IV on the Z sublattice whereas changing the Y sublattice occupation by adding Fe does not lead to an increase of the MAE. Furthermore, we studied the influence of the lattice ratio on the MAE. Showing that small deviations can lead to a doubling of the MAE as in case of Ni_2FeGe. Even though we demonstrate this for a limited set of systems, the findings may carry over to other related systems.

DOI: 10.1103/PhysRevB.98.014411

I. INTRODUCTION

The demand for new magnetic materials is bigger than ever before. Applications are very diverse and comprise permanent magnets for cars and wind turbines, actuators, memory devices, as well as for magnetic cooling, where different applications also demand different technical specifications of the magnetic material. An eminent goal is to identify new materials for magnetic applications. A resource saving and often faster way compared to experiments is computational materials design using *ab initio* methods or atomistic modeling. In principle, two different routes exist: high throughput data mining to find unknown phases or optimization and modification of known structures. In practice, often high throughput studies are carried out with certain constraints on the structure or other properties. Recent examples can be found in Refs. [1,2] where this technique has been used to find new magnetic Heusler compounds. In the latter case, the challenge is to find out on which screw to turn to optimize all relevant properties. From a first-principles point of view, the focus is on three properties as depicted in Fig. 1: the stability of the phase, a ferromagnetic phase with suitable high magnetization, and last but not least the magnetocrystalline anisotropy (MAE) which is crucial for the magnet. As shown in Fig. 1, the properties are related to each other, e.g., a large magnetization without a suitable large MAE will not result in a hard magnet because the coercivity would be too small. Adding atomistic model calculations, further properties such as the Curie temperature can be predicted. However, here the focus is on the basic properties shown on the left side of Fig. 1. Using Ni-based Heusler compounds as model system we discuss the influence of mechanical deformation, alloying, and electronic structure on the basic magnetic properties. Ni-based Heusler compounds are known to show in certain compositions a tetragonal instability which makes them an ideal test system even if the expected Curie temperatures are too low for high-performance magnets. During the last decades, Heusler alloys have been discussed as possible candidates for different magnetic applications, e.g., half-metallic Co_2FeSi for spintronics applications [3–5], rare-earth (RE) free permanent magnets [6,7], or Ni-based actuators [8,9] and magnetocaloric materials [10,11], because their magnetic and electronic properties can be quite easily tuned by composition [12–15]. Depending on the application, the key properties are a high spin polarization, a large magnetocrystalline anisotropy (MAE), a high Curie temperature, or a large magnetic shape memory effect [16]. It has been shown that Co-based Heusler alloys such as Co_2FeSi and Co_2MnSi are half-metallic ferromagnets with magnetic moments following the Slater-Pauling curve and very high Curie temperatures [17,18], Ni-based systems, e.g., Ni_2MnGa, or off-stoichiometric Ni-Mn-Z (Z = Sn, Sb, In) are well known for their shape memory behavior [14,19–21]. Recently, the MAE on Mn-based Heusler alloys has been discussed in view of their suitability for spin transfer torque applications [13]. These systems are ferrimagnetic with a small net moment of 1–2 μ_B but MAE values up to 1 meV/f.u. Furthermore, the search for new rare-earth free or lean ferromagnets has become highly topical since permanent magnets with high MAE are needed en masse, such that cheap and abundant alternatives to the critical RE magnets are needed. Here, we focus on ferromagnetic Heusler systems and in particular on their magnetic properties. The goal is to reveal routes to improve the magnetic properties, in particular the MAE. Even though the absolute values might not reach the MAE of RE or Pt containing materials and the Curie temperatures are expected to be lower than for high-performance magnets, the properties might still be comparable to bonded magnets and ferrites. Thus, Heusler alloys have a huge potential due to the easy tuning by composition and the fact that they are comparably

*heike.herper@physics.uu.se

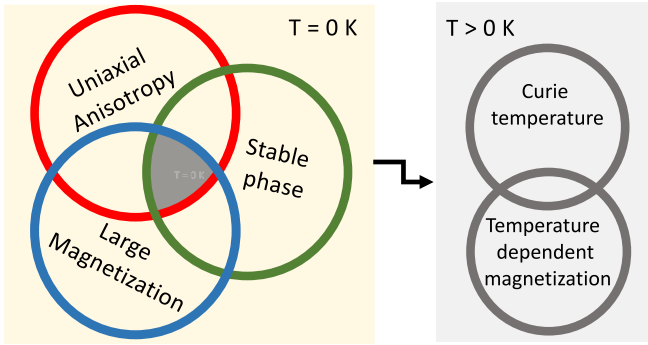

FIG. 1. Computational design of magnetic materials: Basic properties which can be obtained from first-principles calculations ($T = 0$ K) and temperature-dependent quantities which can be determined from additional atomistic modeling.

cheap. Heusler alloys X_2YZ usually crystallize in $L2_1$ structure with point group 225 ($Fm\bar{3}m$ symmetry). It consists of four interpenetrating fcc lattices (see Fig. 2). In ordinary magnetic Heusler alloys, the sublattices A and C are occupied by the metal X whereas another transition metal Y sits on the B site. The last sublattice D is occupied by a main group element Z. In some cases, the occupation of the B and C sublattices is interchanged which leads to a reduction in symmetry, i.e., point group ($216F\bar{4}3m$ symmetry) and the so-called inverse Heusler structure. Which structure is preferred depends in general on the choice of the X and Y elements. For systems with the X element having a higher atomic number than the Y element, the normal $L2_1$ structure is assumed to be the most stable structure whereas inverse-ordered compounds appear for the opposite case. However, we will show that the rule is not strictly followed by Ni_2YZ compounds.

Ni-based Heusler alloys have attracted quite some interest in view of ferromagnetic shape memory alloys (FSMA). They tend to possess a tetragonal instability, i.e., they undergo a martensitic transformation from the high-temperature cubic phase to a low-temperature tetragonal distorted or in some cases to a modulated phase (e.g., 5 M,14 M) [22–24]. Since a tetragonal instability is fundamental for shape memory alloys and magnetocaloric systems, quite some effort has been done to find tetragonally distorted Heusler systems. Furthermore, the tetragonal distortion gives rise to a MAE and its dependence

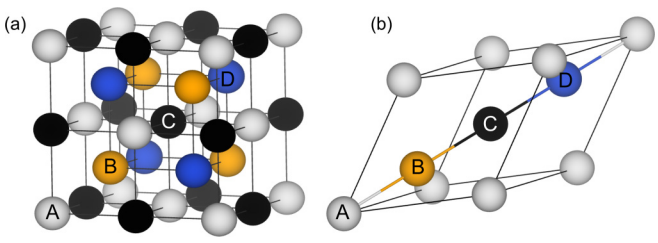

FIG. 2. (a) Unit cell of the cubic $L2_1$ Heusler structure and the corresponding primitive cell (b). In ordinary Heusler alloys with space group 225, the sublattices A and C are occupied by material X, B hosts the Y metal, and the main group element Z is located on the D sublattice. For the inverse Heusler structure (Hg_2CuTi), the occupation of the sublattices B and C is inverted.

on the occupancy of the Y lattice and the choice of the main group element is discussed here. The appearance and stability of the tetragonal state depends on the choice of the Y metal and the main group element. Here, we study Ni_2YZ Heusler alloys with Y = Mn, Fe, Co and Z being an element from main group III or IV with special focus on the magnetic properties, such as the MAE, depending on the Y and Z elements within different density functional theory (DFT) methods. Even though the calculated MAE does not reach the high values of Pt containing Heusler alloys we show that reasonable values due to lattice deformation and out-of plane orientation of the easy axis can be achieved without $5d$ or RE elements and they bear certain potential for magnetic applications.

After a brief description of the computational methods in Sec. II, the stability of the Heusler compounds is discussed in Sec. III. Section IV focusses on the MAE and the magnetic moments, pointing out trends and possible routes to increase the MAE followed by concluding remarks in Sec. V.

II. METHODS

The electronic and magnetic structure of Ni_2YZ Heusler compounds has been investigated within the VASP code [25,26] employing the projected augmented wave (PAW) potentials [27] and the approximations of Perdew, Burke, and Ernzerhof [28] for the exchange correlation functional. The calculations of the stoichiometric systems have been performed within the 4-atomic primitive cell [see Fig. 2(b)]. Systems have been relaxed to forces below 0.01 eV/Å. For calculations within the primitive cell, a 17^3 k-point mesh has been used for structural optimization. Quaternary systems and systems with site disorder have been treated in a 16-atomic cell [Fig. 2(a)] using a k-point mesh of 13^3. The c/a variation has been performed with the same accuracy but the volume and the shape of the unit cell have been fixed if not stated otherwise. We have only considered $L2_1$ order and inverse-ordered systems lower symmetries such as the B2 structure have not been included [29]. It has been shown for Ni_2MnAl that the B2 type phases can also provide a MAE, but it is an order of magnitude smaller than the values discussed in the following sections [30].

To determine the MAE, a full potential linearized augmented plane wave (LMTO) approach has been used employing the RSPT code [31] and spin-orbit coupling was included in all calculations. The optimized structures from the previous VASP investigations served as input for the LMTO code and no further structural optimization has been done. For consistency, the same functional for exchange and correlation has been chosen as before. A mesh of $54 \times 54 \times 54$ points has been used to calculate the MAE from the 4-atomic primitive cells after a k-point convergence check. For the 16-atomic supercells, slightly smaller meshes were used. Within the RSPT code, the wave functions are expanded to $l_{max} = 8$.

The magnetocrystalline anisotropy energy was then calculated from the difference of the total energies for magnetization in [001] and [100] directions $K_1 = E[100] - E[001]$ such that positive energies denote uniaxial anisotropy. For comparison, we also extracted the MAE from Bruno's model which states that the easy axis is parallel to the direction with the largest orbital moment [32]. Originally, this has been used for layered systems which have a quite large MAE at the surface. To

check whether this model holds for our bulk systems, we calculated the difference of the orbital moments $\Delta m_L = m_L[001] - m_L[100]$ such that in case of uniaxial MAE Δm_L is positive.

III. STRUCTURAL STABILITY

A. Cubic vs tetragonal

Heusler alloys with Mn on the Y site and a main group element from group III or IV on the Z site turned out to be regular-ordered alloys with $Fm\bar{3}m$ symmetry in the cubic phase. However, aside from the well-known Ni_2MnGa, only Ni_2MnB possesses a tetragonal instability with $c/a = 1.38$ and a local minimum at $c/a = 0.9$ which was also found in literature [33] [see Fig. 3(a)]. All other investigated Ni_2MnZ alloys have a cubic ground state. The only controversially discussed system is Ni_2MnGe which in agreement with experimental findings by Oksenenko *et al.* [34] turns out to be cubic from the present calculations using PAW potentials, but Luo *et al.* observed tetragonal ground state from DFT calculations with ultra soft pseudopotentials [35]. In addition, calculations of the phonon spectra indicate a softening of the TA_2 mode which also hints to an instability of the cubic phase. A close look at the $E(c/a)$ curve reveals that there is an indication of a shallow local minimum around $c/a = 1.05$ being only 1.22 meV higher in energy than the ground state. Hence, small distortions or different choice of potentials may be sufficient to reverse the order if the local minima and stabilize the tetragonal phase.

In agreement with previous investigations [33,36,37], a tetragonal ground state is observed for nearly all investigated systems if the Y site is occupied with Fe. Exceptions are Ni_2FeIn and Ni_2FeSn which remain cubic [see Fig. 3(b)]. In case of Sn, an indication for a saddle point can be spotted at $c/a = 1.2$ but no real minimum appears for this system. The global minimum for the tetragonal systems occurs at $c/a = 1.35$, only for the B containing system the c/a ratio turned out to be larger than $\sqrt{2}$. Nearly all investigated Ni_2FeZ prefer the ordinary Heusler structure, however, in some cases the energy differences between the ordinary and inverse phases are extremely small [see Fig. 4(a)] and for a summary of all c/a ratios including values from literature we refer to Table I. A prominent example is the Ni_2FeGe system in which the inverse-ordered structure is only 0.2 meV lower in energy than the $L2_1$ ordered phase. An inverse-ordered ground state for Ni_2FeGe has also been observed in previous calculations [37] but contradicts the expectations from Burch's rule as discussed by Kreiner *et al.* [37]. A more detailed study revealed that if we release the constraint of volume conservation the $L2_1$ ordered phase becomes the ground state being 1.86 meV lower in energy than the inverse one [see inset of Fig. 3(b)]. However, since the energy difference is so small, it is hard to determine which structure has to be expected experimentally since such a tiny energy barrier could be overcome at very low temperatures. So far, the Heusler structure was not observed for Ni_2FeGe. From recent high-temperature magnetocalorimetry experiments, there is evidence that at high temperatures a $cP4$ ($L1_2$) structure can be stabilized [38]. However, the Heusler structure might still be produced in thin films.

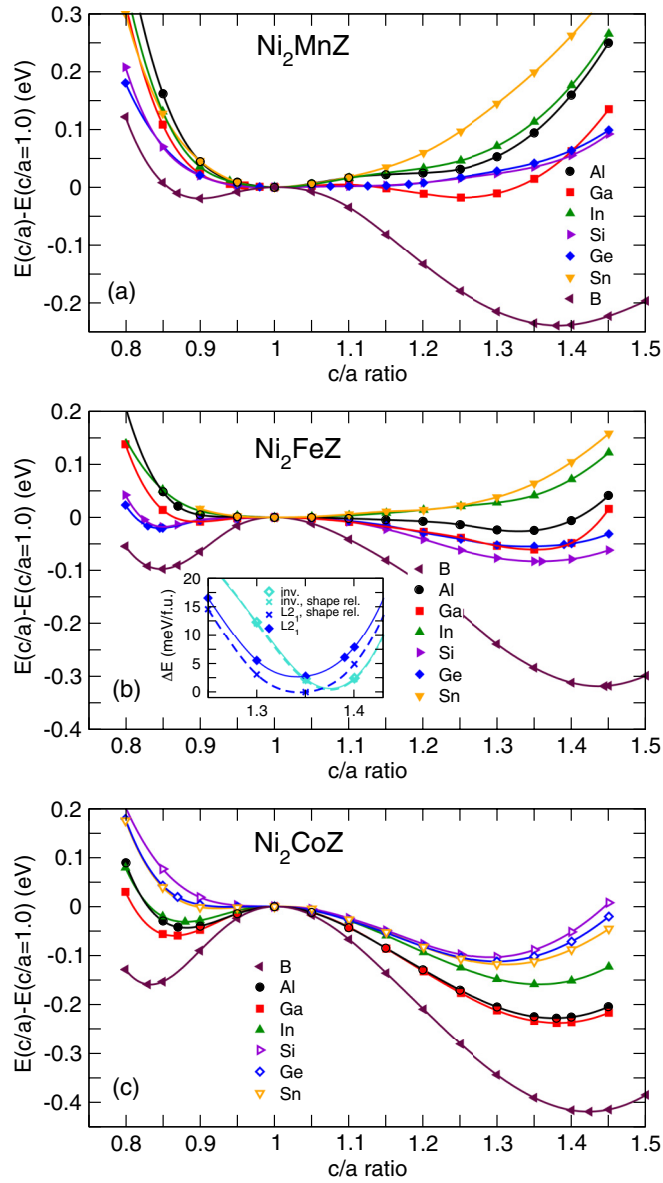

FIG. 3. Energy as function of the c/a ratio for Ni_2YZ Heusler alloys for Z elements with three (B, Al, Ga, In) and four (Si, Ge, Sn) valence electrons. Filled symbols denote normal Heusler structure X_2YZ. Systems which crystallize in the inverse Hg_2CuTi structure are marked by open symbols. Please note the different scales on the y axis for $Y =$ Mn (a). The inset in (b) shows the $E(c/a)$ for $L2_1$ and inverse-ordered Ni_2FeGe in the vicinity of the global minimum.

For Co containing alloys, the symmetry depends on the choice of the Z element, i.e., Z elements from group IV prefer inverse order and the c/a ratio of the global minima is around 1.3 compared to 1.35 (1.38 for Ni_2CoGa) for the $L2_1$ ordered alloys [cf. Fig. 3(c)]. It should be noted that in case of $Y =$ Co the energy difference between the global minimum of the $L2_1$ and inverse order can be analogous to the Fe case quite small [see Fig. 4(a)], i.e., especially for Ni_2CoGa the difference is only -12.55 meV which corresponds to previous findings [45]. Moreover the local minimum of the inverse structure becomes more stable than the one of the $L2_1$ ordered phase such that $E^{\text{inv}}(c/a = 0.92) - E^{\text{L2}_1}(c/a = 0.865) = 37.12$ meV.

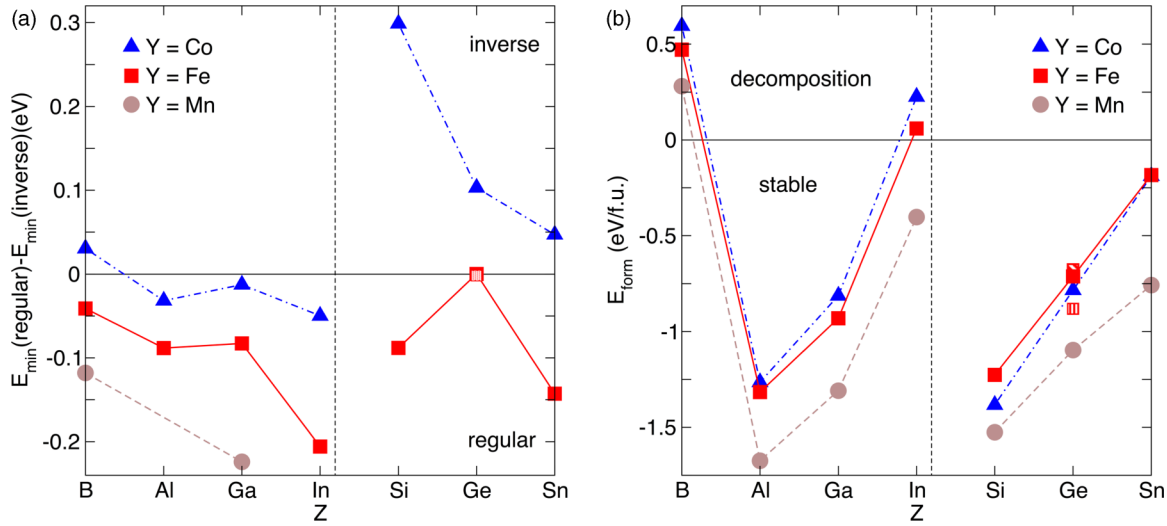

FIG. 4. (a) Calculated energy difference between the $L2_1$ and the inverse-ordered phase for Ni_2FeZ (red squares) and Ni_2CoZ (blue triangles) compounds. For the Mn compounds (brown circles) only the values for the systems with noncubic ground state are shown. (b) Energy of formation for Ni_2YZ Heusler compounds in with Y = Fe (red squares) and Co (blue triangles) as obtained from Eq. (1). Negative values denote systems stable against decomposition. The formation energy of Pd_2FeGe and $(NiPd)_2FeGe$ is given by hatched squares with vertical and diagonal stripes, respectively. Lines should only be viewed as guide to the eye.

Moving from Mn via Fe to Co the energy difference between the cubic and tetragonal phase increases from about 20 meV for Ni_2MnGa to 200 meV for Ni_2CoGa. The Ni_2YB systems are exceptional because the difference in energy between the tetragonal and cubic phases is much larger, i.e., between 240 (Mn) and 400 meV (Co) for the global minima and 20 to 150 meV for the local minima with $c/a < 1$. The difference of the total energies of the high-temperature austenite (cubic) phase and the low-temperature martensite phase (here: tetragonal) can be viewed as a rough measure for the martensitic transition temperature. Barman showed that, with certain restrictions, the $\Delta E = E(c/a)_{\min} - E(c/a = 1.0)$ basically proportional to the martensite temperature, i.e., $k_B T_M$ [46]. Hence, the larger ΔE the higher T_M the tetragonal Ni_2CoZ alloys and Ni_2FeZ (Z = Ge, Ga, Si) phases should be more stable than the well-known Ni_2MnGa which transforms at 206 K to the cubic $L2_1$ structure [47]. Accordingly, the Fe and Co containing systems might be more interesting from the MAE point of view. However, one should keep in mind that the relation between ΔE and T_M is a rough estimation and factors such as the number of valence electrons e/a and the structure (inverse or regular) have some impact. Replacing one sublattice of Ni by Pd leads to a substantial shift of the c/a ratio to larger values ($c/a = 1.42$, see Table III) which is believed to improve the MAE. Aside from the larger c/a ratio, the energy difference between the cubic and the tetragonal phases in $(NiPd)_2FeGe$ is with 0.16 eV/f.u. three times larger than the one of the isoelectronic ternary Ni_2FeGe system which hints to a higher martensite temperature and a larger stability range of the tetragonal phase.

B. Phase stability

In the previous section, the stability of the $L2_1$ vs the inverse Heusler structure has been discussed. However, so far not all investigated systems have been synthesized and it is not known whether the observed ground-state structure is likely to be stabilized experimentally or whether the system decomposes. In order to shed light on this the formation energy E^{form} has been investigated. For a given compound E^{form} can be obtained

TABLE I. Calculated c/a ratios of the global minimum are given for Ni-based Heusler alloys Ni_2YZ. Regular phases are denoted by r, the occurrence on the inverse structure is named i. For comparison value from literature has been added. $e/a(Ni_2Y)$ and $e/a(Z)$ give the number of valence electrons for the metals (Ni and Y) and the main group element on the Z site, respectively.

			Z						
$e/a(Ni_2Y)$	Y		B	Al	Ga	In	Si	Ge	Sn
27	Mn	Here	1.38(r)	1.00(r)	1.25(r)	1.00(r)	1.00(r)	1.00(r)	1.00(r)
27		Other	1.38(r)[33]	1.00(r)[39]	1.27(r)[33]		1.00(r)[40]	1.18(r)[35]	1.00(r)[41]
28	Fe	Here	1.44(r)	1.35(r)	1.35(r)	1.00(r)	1.36(r)	1.35(r)	1.00(r)
28		Other			1.35(r)[33]	1.00(r)[35]		1.30(r)[36]	
						1.30(r)[42]		(i)[37]	
29	Co	Here	1.42(r)	1.38(r)	1.38(r)	1.35(r)	1.30(i)	1.30(i)	1.30(i)
29		Other		1.40(r)[42]	1.38(r)[43]	>1.35[44]		1.30(r)[42]	1.30(r)[42]
	$e/a(Z)$		3	3	3	3	4	4	4

from

$$E^{\text{form}} = E^{\text{Ni}_2YZ} - (2E^{\text{Ni}} + E^{Y} + E^{Z}), \qquad (1)$$

where E^{Ni_2YZ} is the total energy at $T = 0$ K for the ground-state configuration of the Ni_2YZ compound. The other terms E^{Ni}, E^{Y}, and E^{Z} correspond to the ground-state energies calculated for the elemental systems. This can be viewed as a lower boundary and was chosen to handle all systems on the same footing. However, it could be still possible that the compound lies above the convex hull and would decompose in more stable subsystems. No approximations have been made for the ground-state structures of the elements, especially α-Mn ($I\bar{4}3m$ structure) and α-B (experimentally observed structure taken from structure data base ICSD [48,49]) have been used as reference states. Huge differences in the stability of the Heusler compound have been observed for the investigated systems depending on the Z element chosen [see Fig. 4(b)]. Independent from the element on the Y site, all three series show the same trend, compounds with Al and Si are most stable whereas In and B containing compounds tend to decompose. In particular, the B containing systems turned out to be not very likely to occur in nature as a Heusler compound. To our knowledge, all studies discussing Ni_2MnB for example in view of the high spin polarization [33] and possible pressure behavior [50] are based on DFT investigations and so far no experimental verification has been found which agrees with the tendency to decompose observed in this work. In case of In, the trend is less unique. Ni_2MnIn is found to be stable with a formation energy of -0.43 eV whereas Ni_2CoIn decomposes ($E^{\text{form}} = 0.23$ eV) and Fe is in-between with a formation energy being almost zero. In the last case, a reliable conclusion about the stability of this compound cannot be drawn. In case of Ni_2FeIn and Ni_2YSn, the formation energies are small and the argument regarding elemental reference systems might apply. Indeed, these are the systems of the least importance for this paper because they are cubic or provide very small MAE. All other investigated systems turned out to be stable in the Heusler structure being consistent with previous theoretical findings [36,37]. In the next section, the magnetic properties are discussed focusing on the MAE of the stable systems with noncubic ground states.

IV. MAGNETISM

A. Magnetocrystalline anisotropy of Ni_2YZ

We have performed highly accurate MAE calculations within the full potential LMTO method using the optimized structures from previous VASP calculations. Although the investigated compounds have similar c/a ratios, number of valence electrons, and comparable electronic structure, the spread in the MAE values turned out to be quite big. For the ground-state configurations with $c/a > 1$ it reaches from about 0.42 meV/f.u. to almost zero (see Table II). The highest MAE values are achieved for systems with $Y =$ Co and a Z element from group III. In case of Ni_2CoGa and Ni_2CoIn, MAE values of 1.30 MJ/m^3 (0.38 meV/f.u.) and 1.26 MJ/m^3 (0.42 meV/f.u). The MAE for the two above-mentioned $Y =$ Co compounds is about 30% larger than the value obtained for the well-known Ni_2MnGa system which shows an MAE value of about 0.34 meV/f.u. (see Table II). Gruner *et al.* observed an even larger value for $c/a > 1.25$ (MAE = 0.6 meV/f.u.) in Ni_2MnGa [51] using the fully relativistic minimum basis set approach FLPO in the local density approximation [51]. For the Ni_2MnGa system numerous experimental studies exist which have studied the anisotropy. The values spread from $K_u = 1.17 \times 10^6$ erg/cm^3 (0.117 MJ/m^3) to 4–5 $\times 10^6$ erg/cm^3 (0.4–0.5 MJ/m^3) [52–54], depending on the exact composition, and whether single or multivariant samples have been used. In addition, temperature effects play a role and can reduce the size of the magnetocrystalline anisotropy [53]. Our calculated anisotropy energy for Ni_2MnGa is of the same order of magnitude as the experimental values for single crystals [55], but a factor of 3–4 larger which is a quite good agreement regarding the fact that we consider an ideal system at 0 K. Furthermore, the comparison to calculated values in other works shows a spreading in the theoretical data too for example due to the potential used [51]. The calculated values depend partially on the volume, the computational method, and the approximations made, but they give the right order of magnitude. Although the absolute values are sensitive to the computational method, the sign is in our cases robust and it is possible to obtain trends within a series of compounds or alloys calculated on the same footing which can be a guideline for the design of new materials with even larger MAEs.

TABLE II. Calculated magnetic anisotropy energy per formula unit ΔE in meV and K_1 in MJ/m^3. For comparison, the difference of the orbital moments is $\Delta m_L = m_L[001] - m_L[100]$ is also shown. Positive numbers indicate uniaxial anisotropy, whereas negative ones denote planar anisotropy. The anisotropy energies are derived from the differences of the total energies for $\Delta E = E[100] - E[001]$ (for details see Sec. II).

		Z					
Y	MAE	Al	Ga	In	Si	Ge	Sn
Mn	ΔE (meV/f.u.)		−0.338				
	K_1 (MJ/m^3)		−0.967				
	Δm_L (μ_B)		0.029				
Fe	ΔE (meV/f.u.)	0.122	0.090		0.162	0.285	
	K_1 (MJ/m^3)	0.412	0.318		0.574	0.951	
	Δm_L (μ_B)	0.015	0.017		0.007	0.011	
Co	ΔE (meV/f.u.)	−0.381	−0.409	−0.291	0.183	0.119	0.021
	K_1 (MJ/m^3)	−1.013	−1.305	−1.260	0.682	0.418	0.064
	Δm_L (μ_B)	−0.070	0.001	−0.002	0.038	0.018	0.003

While Co has been proven to be advantageous if Z is taken from main group III ($Z =$ Al, Ga, In) Ni_2CoZ compounds with Z being Si, Ge, or Sn are less promising. The calculated MAE values are in agreement with Ref. [56] significantly smaller, e.g., 0.42 MJ/m^3 in case of Ni_2CoGe. In contrast to Ni_2CoGa(In), the easy axis is out of plane. However, even though these systems are uniaxial ferromagnets, the magnetic properties are less good due to the inverse order. One reason is the change in the local coordination of the magnetic Co atom which has 4 Ni and 4 Z atoms instead on 8 Ni atoms (see Sec. IV). Therefore, the magnetization of the inverse-ordered systems is smaller compared to the $L2_1$ type systems. In addition, this effects the lattice structure and leads to smaller c/a values for the ground-state configuration.

Taking everything into consideration, i.e., MAE, magnetic moments, and phase stability Ni_2FeZ (Z = Si, Ge) seem to be advantageous. Both systems provide a tetragonal ground state and an easy-axis MAE. The largest MAE occurs for Ni_2FeGe 0.95 MJ/m^3 (see Table II). This is comparable to the findings for the Mn-based tetragonal Heusler systems [13]. Since for Ni_2FeGe the $L2_1$ and inverse-ordered structure are very close in energy (see discussion in Sec. III), the MAE of the inverse-ordered system has also been investigated. It turned out to be by a factor of 2 smaller than the one of the regular Heusler compound ($c/a = 1.3$, MAE = 0.54 MJ/m^3). This observation is in line with the findings for the inverse-ordered Ni_2CoZ compounds. Summarizing, the largest values for the MAE have been predicted for Ni_2CoZ (Z = Ga, In) and Ni_2FeGe which have the same number of valence electrons per f.u. ($e/a = 32$).

Hence, the calculation of the MAE from total energies is quite costly and it is tempting to find a cheaper way. Bruno has derived an alternative expression from second-order perturbation theory [32] which states that the MAE will point in the direction of the largest orbital moment and is proportional to the difference of the orbital moments between easy and hard axes. Here, the orbital moments along [001] and [100] directions have been taken into account. Apparently, this model holds for most of the cases discussed here, the correct orientation of the MAE is predicted for all systems but Ni_2CoGa and Ni_2MnGa. In case of Ni_2CoGa, the difference of the orbital moments nearly vanishes (see Table II) because the orbital moments of Co and Ni are counteracting. Whereas Co moments are larger in [100] direction, the orbital moments of Ni are larger in [001] direction. In case of Ni_2MnGa, the model seems to fail since all orbital moments, Ni and Mn, are larger for [001] orientation even though the calculated MAE is planar in agreement with experimental findings. Also, the trends depending on e/a are not reproduced well. Thus, the model is not really suitable for this type of systems with relatively small orbital moments. The model was originally developed for layered systems where the MAE and spin-orbit effects especially at the interfaces can be quite large. A recent study for Fe films and clusters showed that the model works fine for the trends at the interface but can fail in the center of the film where the MAE is smaller [57].

From the c/a variation discussed in Sec. III, it is obvious the tetragonal distorted systems have not only a global minimum at $c/a > 1$ but also a local minimum for compressed systems with $c/a < 1$. In some cases, the global minimum is not reached and the local minimum $c/a < 1$ appears. The MAE values for the local minima at $c/a < 1$ tend to be smaller which is at least partially related to the smaller deviation from the cubic structure. For example, in case of Ni_2CoGa, the system with the highest MAE for $c/a > 1$, the MAE for the local minimum ($c/a = 0.87$) is with -0.10 MJ/m^3 by a factor of 10 smaller (see Fig. 5). On the other hand, moving from elongation to compression is accompanied by a change from easy plane to easy axis anisotropy. This has been reported before for Ni-based Heusler compounds such as Ni_2MnGa [51] and $Ni_2Mn_{1.25}In_{0.75}$ [20]. For Ni_2MnGa, a MAE of 0.186 meV/f.u. ($c/a = 0.94$) is achieved which is in good agreement with the full potential augmented plane wave calculations by Enkovaara *et al.* (MAE = 0.18 meV/f.u.) [58]. Due to the smaller tetragonal distortion, the size of the MAE falls usually behind the one of the previously discussed case for $c/a > 1$. An exception is Ni_2FeGe [MAE($c/a = 0.85$) = 0.20 meV] system where the change is comparably smaller. This underlines that the c/a ratio is not the only determining factor. No or very tiny MAE values are obtained for the inverse-ordered Ni_2CoZ systems at $c/a < 1$ since the magnetic moment vanishes with decreasing c/a (Z = Si, Ge) and the tetragonal distortion of the local minimum is small (Z = Sn, $c/a = 0.92$, MAE = -0.004 meV) (see Supplemental Material for MAE values of the local minima with $c/a < 1$ [59]).

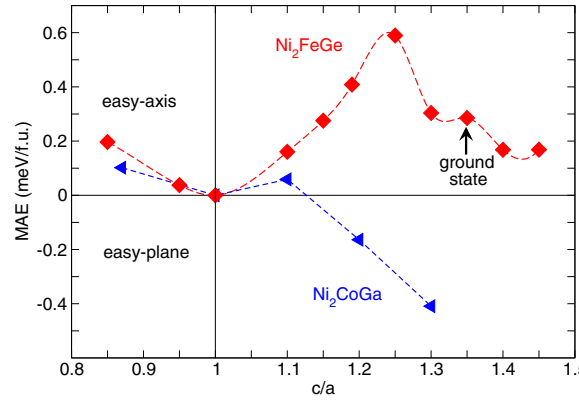

FIG. 5. Dependence of the magnetocrystalline anisotropy on the lattice ratio c/a for Ni_2FeGe (red diamonds) and Ni_2CoGa (blue triangles) as obtained from RSPT. In case of Ni_2FeGe, no sign change, i.e., rotation of the MAE from easy axis to planar is observed depending on the c/a ratio, whereas Ni_2CoGa undergoes the typical change from planar (negative values) to uniaxial when the c/a changes from $c/a > 1$ to $c/a < 1$.

B. Possible routes to tailor the magnetocrystalline anisotropy

It is fair to say that some Ni-based Heusler compounds reveal promising MAEs, but the most interesting systems (in view of large MAE values) have positive formation energies, are easy-plane systems, or could not be synthesized as bulk systems even if predicted by theory to be stable. Here, we focus on possible ways how to tailor the size and the sign of the MAE and simultaneously stabilize the tetragonal phase. Special focus will be on the effect of lattice deformation, forming quaternary compounds to turn easy-plane magnets into easy-axis systems. Knowing that heavier materials provide a larger spin-orbit coupling and are therefore likely to possess also a larger anisotropy compared to 3d materials we consider also the influence of 4d element replacements of Ni. In this paper, we have studied in particular Pd which is isoelectronic to Ni.

1. Changing the lattice geometry

Changing the lattice distortion from elongation to compression of the c axis is in many Heusler-type compounds accompanied by a rotation of the easy axis from in-plane to out-of-plane orientation [20,51]. The MAE often varies quasilinear with c/a far away from the minima and slightly larger variations in the vicinity of the minima as shown in

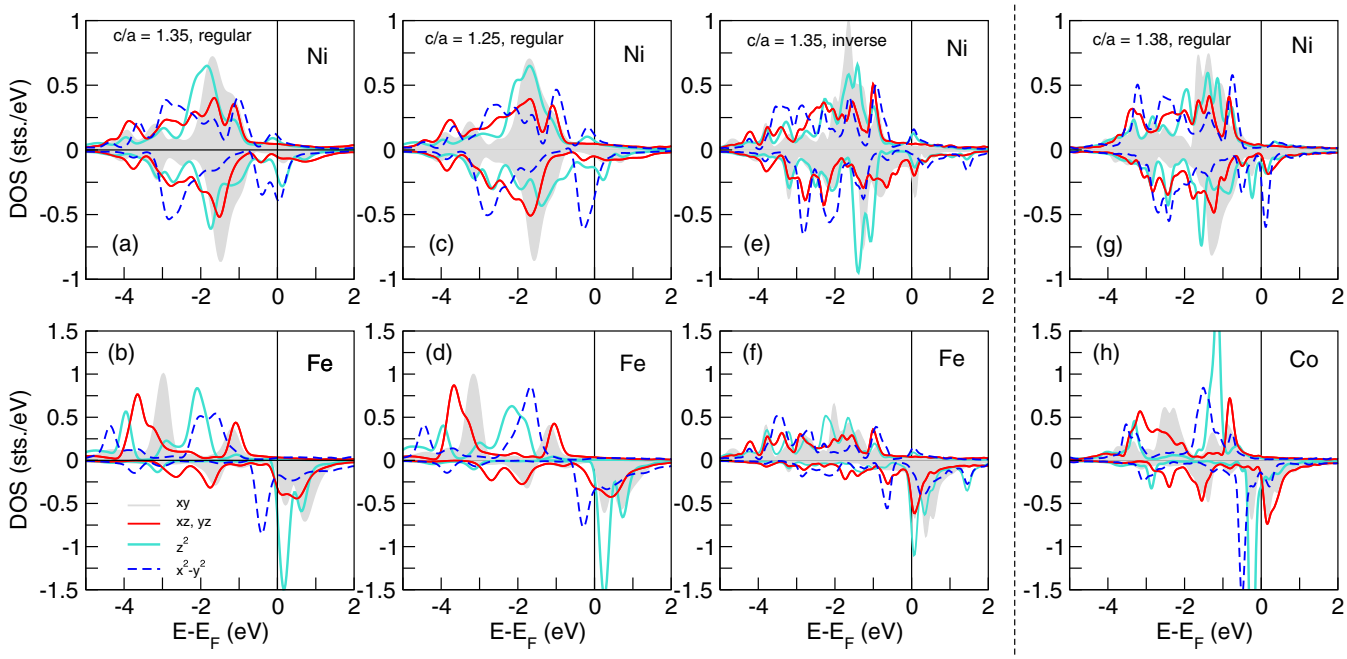

FIG. 6. Calculated orbital resolved density of states of Ni_2FeGe (a)–(f) and Ni_2CoGa (g)–(h). The upper row shows the Ni d states of the systems, whereas the Fe and Co d states are given in the bottom row. In (a) and (b), the DOS of the ground-state configuration of Ni_2FeGe ($c/a = 1.35$) is given, (c) and (d) denote the DOS of the system with the highest MAE ($c/a = 1.25$). The DOS for the ground state of the inverse-ordered (Hg_2CuTi structure) system Ni_2FeGe ($c/a_i = 1.35$) is given in (e) and (f). For Ni_2CoGa, only the ground-state configuration with $c/a = 1.38$ is given [see (g) and (h)].

Fig. 5 for Ni_2CoGa. Another example for an off-stoichiometric Ni-based Heusler system can be found in Ref. [20]. Such a change in the orientation of the easy axis is not observed for the systems which possess an out-of-plane axis for $c/a > 1$ (see Supplemental Material [59] and Fig. 5). A strong nonlinear c/a dependence occurs in case of Ni_2FeGe. Reducing the tetragonal distortion by about 10% ($c/a = 1.25$) leads to a 100% increase of the MAE compared to the ground state ($c/a = 1.35$) (cf. Fig. 5). With 1.96 MJ/m^3 the MAE is even larger than the values obtained for Ni_2CoZ and what is even more important the system is uniaxial. The large MAE and the possibility to tune by small lattice distortions might make this system interesting in view of applications. However, to our knowledge it has not been successfully synthesized as a bulk system in $L2_1$ structure, but one might think to stabilize a structure as a thin film where the c/a ratio could be optimized by dopants or deposition or the choice of the substrate. The remaining question is what drives the changes in the magnetic behavior and how is it related to changes in the electronic structure? Comparing the orbital resolved density of states (DOS) of the tetragonal ground state ($c/a = 1.35$), the squeezed structure ($c/a = 1.25$), and the ground state ($c/a_i = 1.35$) of the inverse-ordered system, characteristic changes of the DOS in the vicinity of the Fermi level can be observed [see Figs. 6(a)–6(f)]. It has been shown that the states next to the Fermi energy play a crucial role for the MAE and allow conclusions on its orientation [32]. Furthermore, the findings by van Vleck [60] state that the microscopic origin of the MAE due to the spin-orbit (LS) coupling in the system and in second order-perturbation theory lead to the well-known formula for the energy change due to spin-orbit coupling

$$\Delta E_{\mathrm{LS}} = \xi^2 \frac{|\langle k|\mathbf{LS}|n\rangle|^2}{E_k - E_n}, \tag{2}$$

where n and k describe unoccupied and occupied states near the Fermi level and ξ is the spin-orbit coupling strength. While the energy difference in the denominator of Eq. (2) influences the size of the energy change, the matrix elements in the enumerator determine the orientation of the MAE. Considering only the d states of the magnetically dominant transition metal, Fe or Co, the uniaxial MAE of Ni_2FeGe can be understood from the fact that the states above and below the Fermi level have large xy and x^2-y^2 contributions [the z^2 states do not contribute since the matrix element with z^2 and (x, y) vanishes, see Ref. [61]].

Reducing the c/a ratio from 1.35 to 1.25 leads to a shift of the Fe d orbitals or more precisely a reduction of the energy difference between the highest occupied and lowest unoccupied states which determine the energy difference in Eq. (2) [compare Figs. 6(b) and 6(d)]. In the $c/a = 1.25$ case, ΔE_{LS} is 0.05 eV smaller compared to $c/a = 1.35$ and hints for a larger spin-orbit coupling and consequently a larger MAE. The same argument holds for the inverse-ordered Ni_2FeGe system [Fig. 6(f)]; here ΔE_{LS} between the states with nonvanishing matrix elements is about 0.04 eV larger than for the ground state [Fig. 6(b)] and a smaller MAE could be expected. This corresponds to the findings from the calculations of the MAE from the total energy differences. The MAE of these three systems follows the trend predicted by perturbation theory, i.e., it increases from inverse structure ($c/a_i = 1.35$) which

has a negligible MAE of about 0.09 MJ/m^3 over the ground state (about 1 MJ/m^3) to the distorted configuration with 1.96 MJ/m^3. It should be noted that despite the huge changes in size, the MAE remains always uniaxial for this system.

From the same line of arguments, we can understand the behavior of Ni_2CoGa. Here, the n and k states close to the Fermi level have different characters mostly because Co has one d electron more than Fe. Here, z^2 and (xz, yz) states contribute to the energy in Eq. (2) which favor planar anisotropy in agreement with the findings in Sec. IV A. The size of the MAE is again reflected in the small distance (0.15 eV less than for the Ni_2FeGe ground state) between occupied and unoccupied minority-spin states [see Figs. 6(g) and 6(h)].

2. *Quaternary compounds*

While in the previous section structural changes within one system were discussed we will focus here on alloying on one sublattice to improve the magnetic properties. Two examples have been chosen. In the first case, the Z sublattice is used to improve the MAE of Ni_2CoZ. On the one hand, from Table II it is conclusive that Ni_2CoGa and Ni_2CoIn have the largest MAE values, unfortunately it is not a uniaxial anisotropy and as discussed previously the In compound is not expected to be stable at low temperatures (cf. Sec. III). On the other hand, the inverse-ordered Ni_2CoGe has a much smaller MAE but it is uniaxial and the compound is according to our survey stable in the Hg_2CuTi structure. Therefore, it seems a natural choice to replace In partially by Ge which means increasing the e/a. Here, In has been chosen over Ga because of the larger atomic number the spin-orbit (LS) coupling is expected to be larger and this in turn should counteract the reduction of the MAE which is expected due to Ge. We replaced 25% and 50% of In by Ge using a 16-atomic supercell (see Sec. II). The quaternary $Ni_2Co(In_{0.5}Ge_{0.5})$ compound turns out to be stable (cf. inset of Fig. 7) and as for Ni_2CoIn the inverse-ordered structure is lower in energy. Compared to Ni_2CoIn or Ni_2CoGa, the MAE is with 0.61 MJ/m^3 by a factor of 2 smaller (50% Ge), but what is more important is that the partial replacement of In by Ge has led to an easy axis anisotropy (see Fig. 7). Smaller Ge concentrations would give smaller MAE values, but the magnetic anisotropy remains uniaxial as in the original compound Ni_2CoIn. Furthermore, for Ge concentrations equal to 25% or less, the quaternary compound decomposes (see inset in Fig. 7). Summarizing, by mixing Ni_2CoGe and Ni_2CoIn one gets basically the best of both systems, i.e., a stable phase with uniaxial MAE. However, the magnetic moment of the quaternary compound is reduced compared to Ni_2CoIn which is a tribute to the inverse-ordered structure in which the moments are smaller compared to regular Heusler compounds (see also Sec. IV). Although, replacing In partially by Ge stabilizes the compound and improves the magnetic properties, i.e., turns the system in a uniaxial magnet, similar behavior might be expected by using Si instead of Ge since the preconditions are very similar but the ternary Ni_2CoSi compound shows an even larger uniaxial MAE. However, substituting 50% of In by Si leads to an inverse-ordered tetragonal structure with $c/a < 1$, namely, $c/a = 0.905$ and a local minimum at $c/a = 1.2$ [see Supplemental Material for $E(c/a)$ curves depending on the In and Ge(Si) concentration [59]]. In contrast to the previous case

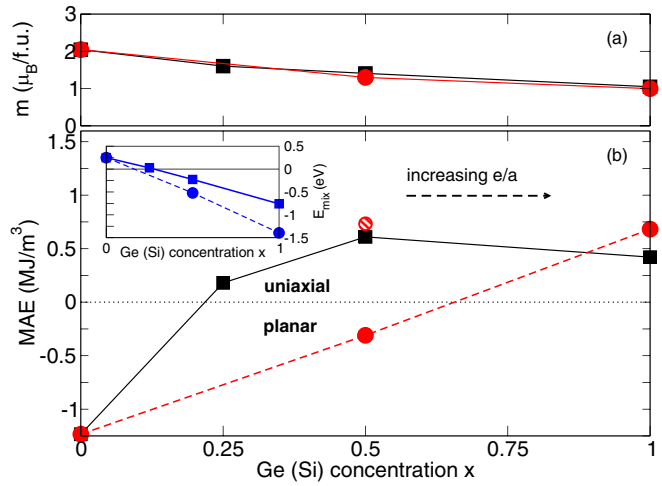

FIG. 7. Calculated magnetic moments per formula unit (a) and magnetocrystalline anisotropy (b) depending on the impurity concentration, i.e., the valence electron number e/a for $Ni_2CoIn_{1-x}Z_x$ with Z = Ge (squares) and Si (circles). The inset at the top left in (b) gives the formation energy and stabilization of the system with increasing Ge and Si content, respectively. The inset on the bottom of the right-hand side shows the supercell (16 atoms) used for the quaternary systems, here 50% of In have been substituted by Ge. The hatched circle corresponds to the MAE of the local minima of $Ni_2CoIn_{0.5}Si_{0.5}$ ($c/a = 1.2$).

with Si, the MAE remains planar if 50% of Ge are replaced by Si (see Fig. 7). The MAE changes quasilinearly from Ni_2CoIn to Ni_2CoSi leading to a planar MAE of 0.31 MJ/m^3 for $Ni_2CoIn_{0.5}Si_{0.5}$. This difference between Si and Ge seems to be related to the change of the neighbor distances in the quenched phase ($c/a < 1.0$), hence, for the local minimum ($c/a = 1.2$) the situation is the same as in the In case. The MAE is uniaxial being slightly larger than for the ternary parent system Ni_2CoSi (see hatched circle in Fig. 7).

In the second case, we followed the same line of argument but tailoring the occupation of the Y sublattice instead. In this case, we keep the Z element fixed. In our case we have chosen Z = Al. Both ternary compounds are regular Heusler systems with a tetragonal ground state and are stable according to Fig. 4. Aiming to increase the MAE of Ni_2FeAl, Fe has been partially replaced by Co since Ni_2CoAl has a larger MAE which is unfortunately planar (see Table II). However, instead of improving the magnetic properties as in the previous example, the MAE almost vanishes. For $Ni_2Fe_{0.75}Co_{0.25}Al$ calculated in a 16-atom supercell, the MAE remains uniaxial but decreases to a value <0.1 MJ/m^3.

3. *Isoelectronic replacement of Ni*

It has been pointed out be van Vleck [60] and later also discussed in Bruno's model [32] that the MAE is directly related to the spin-orbit coupling strength ξ of a system and knowing that ξ is related to the atomic number by $\xi \sim Z^4$, i.e., aiming for a large MAE heavy elements are preferable. Therefore, we replaced Ni partially by Pd assuming that an isoelectronic exchange will improve the magnetic properties, especially the MAE, and leave the other properties such as the phase stability unchanged. As test system we have

TABLE III. Structure data and magnetic properties for a series of isoelectronic Heusler compounds $Ni_{1-x}Pd_xFeGe$. Note the magnetic moments shown here are the total magnetic moments including the orbital moment as obtained from full potential DFT calculations using RSPT [31]. Positive sign for the MAE indicates uniaxial anisotropy.

System	c/a	Volume (Å^3/f.u.)	m_{tot} (μ_B/f.u.)	MAE (MJ/m^3)
Ni_2FeGe	1.35	48.00	3.50	0.95
$(NiPd)_2FeGe$	1.42	53.82	3.40	0.97
Pd_2FeGe	1.38	58.86	3.24	0.61

chosen Ni_2FeGe which has already a suitable MAE of about 1 MJ/m^3. Half of the Ni atoms in this compound have been replaced by Pd and calculations have been performed using a 16-atomic supercell. For comparison, we have also studied the Ni-free system Pd_2FeGe. As expected, the isoelectronic replacement has no significant influence on the phase stability. The formation energies are with −0.676 eV $(NiPd)_2FeGe$ and −0.881 eV (Pd_2FeGe) in the same range as for Ni_2FeGe (see hatched symbols in Fig. 4). Inducing Pd in the Heusler compound to replace Ni should have only minor influence on the electronic structure (isoelectronic) and preserve to uniaxial MAE. This is indeed observed the MAE remains uniaxial and the volume increases due to the larger Pd atom (see Table III). Replacing 50% of the Ni atoms (16-atom supercell) leads to an increase of the volume per f.u. by 12%, but unfortunately the MAE does not change much. It basically remains constant at 0.97 MJ/m^3 (cf. Table III) but would increase the prize by a factor of 1400. So, the replacement of Ni by Pd would not only be inefficient but also incredibly expensive.

C. Magnetic moments

The magnetic moments of Heusler alloys show usually Slater-Pauling–type behavior, i.e., their total magnetic moments depend linearly on the number of valence electrons. First demonstrated for $L2_1$ ordered Co-based half-metallic ferromagnets, similar behavior has been observed for related systems. In case of the half-metallic Co-based compounds, the magnetic moments are given by $M = N_v$-24 with N_v being the number of valence electrons per formula unit [62] which gives integer magnetic moments for stoichiometric ordered systems. It has turned out that this rule can be generalized for many classes of Heusler alloys. Half-metallic Heusler alloys X_2YZ with X being an early 3d transition metal obey, depending on the Y and Z constituents, slightly different rules, namely, $M = N_v - 18$ and $M = N_v - 28$ [63]. For $Ni_2Mn_{1-x}Ga_x$ alloys, Dannenberg proposed a $M = 34 - N_v$ behavior of the total magnetic moment [45]. As shown in Fig. 8 also all Ni-based Heusler alloys with a Z element from main group III obey this rule. Adding electrons to the system by occupying the Z sublattice with an element from main group IV increases the spin moments such that they follow the rule $M = 35 - N_v$. However, one should keep in mind that not the number of valence electrons N_v decides which rule the system obeys, but the choice of the Z element. Taking, for example, Ni_2CoGa and Ni_2FeGe, both systems have $N_v = 32$ but obey different rules, i.e., the Fe compound has a higher magnetic moment (see

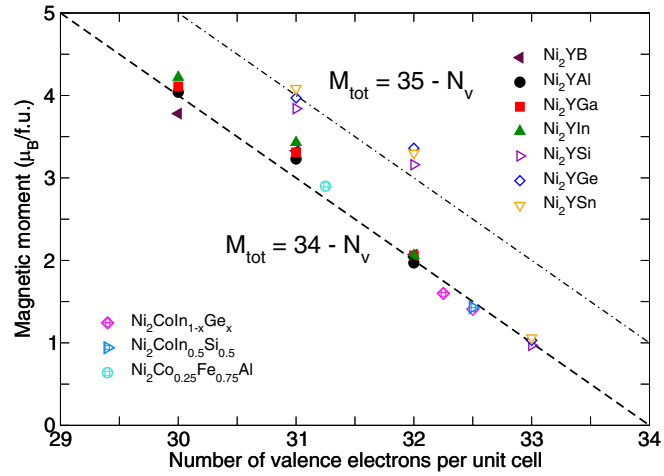

FIG. 8. Total magnetic moments of the ground state. The value of the cubic ($c/a = 1.0$) structure is given in brackets. All values are in μ_B/f.u. The dashed line marks the 34-N_v rule for shape memory alloys as suggested by Dannenberg *et al.* [45] whereas the magnetic moment for the inverse-ordered systems with the Z element being from group IV follows shows a 35-N_v behavior (dashed-dotted line). Inverse-ordered systems including the quaternary ones (hatched symbols) follow the dashed line since their moment is reduced due to the reversed NN positions.

Fig. 8). This is related to the fact that the DOS at the Fermi level is mostly determined by the 3d states of the transition metals (cf. Fig. 6). In case of Ni_2CoGa, the minority-spin channel is more occupied and therefore the spin moment smaller compared to the Fe compound. A peculiarity occurs for the inverse-ordered Ni_2CoZ systems with Z being an element from group IV. We have argued in the previous sections that inverse-ordered Heusler compounds for the same type of compound have smaller magnetic moments due to different local order. This observation can be quantified as shown in Fig. 8. Obviously, Ni_2YZ compounds with Z from main group IV follow only the $M = 35 - N_v$ rule if they are of $L2_1$ type. The inverse-ordered Ni_2CoZ (Z from group IV) obey the $M = 34 - N_v$ rule instead (see open symbols for $N_v = 33$). The same observation is made for the inverse-ordered quaternary systems (hatched symbols in Fig. 8).

V. CONCLUSION

Ni-based Heusler compounds Ni_2YZ have been used as an example to study different routes to improve the magnetic properties with special focus on the MAE. The magnetic moments of the systems follow modified Slater-Pauling laws, showing clearly that the magnetic moment of the inverse-ordered systems is systematically lower than for regular Heusler compounds.

Out of the 21 studied systems, 14 possess a noncubic ground state being a prerequisite for a finite MAE. From these candidate systems the ones with Co on the Y sublattice turned out to be most interesting. In Ni_2CoZ compounds the tetragonal phase turned out to be most stable, i.e., the transformation to the cubic austenite phase will occur at higher temperature as for example for Ni_2MnGa. However, the Ni_2CoZ (Z = In,

Ga) systems with the largest MAE turned out to have a planar MAE and/or are even unstable. We could show that this could be cured by combining them with inverse-ordered Ni_2CoGe which has a uniaxial MAE. Using Si instead of Ge turned out not to be successful because the tetragonal phase in Ni_2CoSi has $c/a < 1$. For the local minimum at $c/a = 1.2$ the same effect as for Ge is observed. Hence, the phase can be stabilized by adding valence electrons (replacing In partially by Si or Ge) but to improve the magnetic properties also the lattice structure of the ternary phases has to match. Aiming to increase the uniaxial MAE of Ni_2FeAl we used the same strategy, but replacing partially Fe by Co since Ni_2CoAl as a larger (planar) MAE. However, it turned out that 25% Co of the Fe sublattice reduce the MAE drastically. This is not completely unexpected since changing the coordination and magnetism can lead to a reduction of the MAE.

Another way to improve the MAE could be the use of heavier elements, which possess larger spin-orbit coupling. To test this for our set of systems, we selected the ternary system with the largest uniaxial MAE, Ni_2FeGe. Partial isoelectronic replacement of Ni by Pd showed only minor effect on the MAE because, due to Pd the volume increases and the magnetic moments slightly decrease, both facts counteract to an increase of the MAE.

The MAE also changes with the lattice ratio such that one can think to tailor the MAE by stress or strain. Basically, this c/a dependence has been discussed for Ni_2MnGa and other systems in literature before. Most systems show a quasilinear behavior with a sign change at or close to $c/a = 1$. However, in case of Ni_2FeGe the MAE remains uniaxial for all lattice ratios between 0.85 and 1.45. For this particular system, small deviations from the equilibrium c/a boost the MAE from about 1 to 2 MJ/m^3. Similar behavior is expected for other Ni_2FeZ compounds since the orientation of the MAE for the ground state and the local minimum at $c/a < 1.0$ are the same. The MAE values discussed in this paper have been obtained from total energy differences and from the differences of the orbital moments (Bruno's model). The latter turned out not to give always the right orientation or trend of the MAE, which might be related to the quite small orbital moments in these systems.

Concluding, for the systems under consideration we discussed different routes to manipulate the MAE, e.g., creating quaternary compound by doping or by lattice deformation. Both routes turned out to be successful under certain conditions and MAE values of 1 MJ/m^3 and higher could be achieved. Limitations for practical use are the height of martensite temperature and the Curie temperature. Especially the Curie temperature has recently been predicted to be quite low in some of the systems. However, although we have limited ourselves to Ni-based Heusler compounds, we believe that the results can carry over to other Heusler compounds and with this also the finite-temperature properties might be improved.

ACKNOWLEDGMENTS

H.C.H. would like to thank M. Werwinski and Y. Kvashnin for helpful discussions and support. I acknowledge financial support by the EU through the Horizon 2020 framework programme NOVAMAG (Grant No. 686056) and STandUP for energy. The computations were performed on resources provided by the Swedish National Infrastructure for Computing (SNIC) at HPC2N (Umeå), NSC (Linköping), and PDC (KTH Stockholm).

[1] S. Sanvito, C. Oses, J. Xue, A. Tiwari, M. Zic, T. Archer, P. Tozman, M. Venkatesan, M. Coey, and S. Curtarolo, Sci. Adv. **3**, e1602241 (2017).
[2] J. Balluff, K. Diekmann, G. Reiss, and M. Meinert, Phys. Rev. Mater. **1**, 034404 (2017).
[3] M. Meinert, J.-M. Schmalhorst, M. Glas, G. Reiss, E. Arenholz, T. Böhnert, and K. Nielsch, Phys. Rev. B **86**, 054420 (2012).
[4] J. Sagar, C. N. T. Yu, L. Lari, and A. Hirohata, J. Phys. D: Appl. Phys. **47**, 265002 (2014).
[5] S. Wurmehl, J. T. Kohlhepp, H. J. M. Swagten, B. Koopmans, M. Wójcik, B. Balke, C. G. F. Blum, V. Ksenofontov, G. H. Fecher, and C. Felser, Appl. Phys. Lett. **91**, 052506 (2007).
[6] J. Kiss, S. Chadov, G. H. Fecher, and C. Felser, Phys. Rev. B **87**, 224403 (2013).
[7] P. Nordblad, Nat. Mater. **14**, 655 (2015).
[8] A. Ayuela, J. Enkovaara, K. Ullakko, and R. M. Nieminen, J. Phys.: Condens. Matter. **11**, 2017 (1999).
[9] E. Kalimullina, A. Kamantsev, V. Koledov, V. Shavrov, V. Nizhankovskii, A. Irzhak, F. Albertini, S. Fabbrici, P. Ranzieri, and P. Ari-Gur, Phys. Status Solidi C **11**, 1023 (2014).
[10] J. Ren, H. Li, J. Yu, S. Feng, and H. Zheng, J. Alloys Compd. **634**, 65 (2015).
[11] V. D. Buchelnikov and V. V. Sokolovskiy, Phys. Met. Metallogr. **112**, 633 (2011).
[12] T. Graf and C. Felser, in *Heusler Compounds at a Glance Heusler Compounds at a Glance*, edited by C. Felser and G. Fecher (Springer, Berlin, 2013), pp. 1–13.
[13] J. Winterlik *et al.*, Adv. Mater. **24**, 6283 (2012).
[14] V. D. Buchelnikov, V. V. Sokolovskiy, H. C. Herper, H. Ebert, M. E. Gruner, S. V. Taskaev, V. V. Khovaylo, A. Hucht, A. Dannenberg, M. Ogura, H. Akai, M. Acet, and P. Entel, Phys. Rev. B **81**, 094411 (2010).
[15] M. Ye, A. Kimura, Y. Miura, M. Shirai, Y. T. Cui, K. Shimada, H. Namatame, M. Taniguchi, S. Ueda, K. Kobayashi, R. Kainuma, T. Shishido, K. Fukushima, and T. Kanomata, Phys. Rev. Lett. **104**, 176401 (2010).
[16] P. Entel, A. Dannenberg, M. Siewert, H. C. Herper, M. E. Gruner, D. Comtesse, H.-J. Elmers, and M. Kallmayer, Metall. Mater. Trans. A **43**, 2891 (2011).
[17] S. Wurmehl, G. H. Fecher, H. C. Kandpal, V. Ksenofontov, C. Felser, H.-J. Lin, and J. Morais, Phys. Rev. B **72**, 184434 (2005).
[18] I. Galanakis, P. Mavropoulos, and P. H. Dederichs, J. Phys. D: Appl. Phys. **39**, 765 (2006).
[19] M. Siewert *et al.*, Appl. Phys. Lett. **99**, 191904 (2011).

[20] B. Krumme, A. Auge, H. C. Herper, I. Opahle, D. Klar, N. Teichert, L. Joly, P. Ohresser, J. Landers, J. P. Kappler, P. Entel, A. Hütten, and H. Wende, Phys. Rev. B **91**, 214417 (2015).

[21] P. Klaer, H. C. Herper, P. Entel, R. Niemann, L. Schultz, S. Fähler, and H. J. Elmers, Phys. Rev. B. **88**, 174414 (2013).

[22] M. A. Uijttewaal, T. Hickel, J. Neugebauer, M. E. Gruner, and P. Entel, Phys. Rev. Lett. **102**, 035702 (2009).

[23] K. Endo *et al.*, Mater. Sci. Forum **684**, 165 (2011).

[24] Y. Tanaka, S. Ishida, and S. Asano, Mater. Trans. **45**, 1060 (2004).

[25] G. Kresse and J. Furthmüller, Comput. Mater. Sci. **6**, 15 (1996).

[26] G. Kresse and J. Hafner, Phys. Rev. B **49**, 14251 (1994).

[27] P. E. Blöchl, Phys. Rev. B **50**, 17953 (1994).

[28] J. P. Perdew, K. Burke, and M. Ernzerhof, Phys. Rev. Lett. **77**, 3865 (1996).

[29] I. Galanakis and E. Şaşioğlu, Appl. Phys. Lett. **98**, 102514 (2011).

[30] E. Simon, J. G. Vida, S. Khmelevskyi, and L. Szunyogh, Phys. Rev. B **92**, 054438 (2015).

[31] J. M. Wills, M. Alouani, P. Andersson, A. Delin, O. Eriksson, and O. Grechnyev, *Full-Potential Electronic Structure Method*, Vol. 167 of Springer Series in Solid State Science (Springer, Berlin, 2010).

[32] P. Bruno, Phys. Rev. B. **39**, 865 (1989).

[33] Y. Qawasmeh and B. Hamad, J. Appl. Phys. **111**, 033905 (2012).

[34] V. A. Oksenenko, L. N. Trofimova, Y. N. Petrov, Y. V. Kudryavtsev, J. Dubowik, and Y. P. Lee, J. Appl. Phys. **99**, 063902 (2006).

[35] H. Luo, F. Meng, G. Liu, H. Liu, P. Jia, and E. Liu, Intermetallics **38**, 139 (2013).

[36] M. Gilleßen and R. Dronskowski, J. Comput. Chem. **31**, 612 (2010).

[37] G. Kreiner, A. Kalache, S. Hausdorf, V. Alijane, J.-F. Qian, G. Shan, U. Burkhardt, S. Ouardi, and C. Felser, Z. Anorg. Allg. Chem. **640**, 738 (2014).

[38] M. Yin, P. Nash, W. Chen, and S. Chen, J. Alloys Compd. **660**, 258 (2016).

[39] J. Enkovaara, A. Ayuela, J. Jalkanen, L. Nordström, and R. M. Nieminen, Phys. Rev. B **67**, 054417 (2003).

[40] Q.-L. Fang, J.-M. Zhang, X.-M. Zhao, K.-W. Xu, and V. Ji, J. Magn. Magn. Mater. **362**, 42 (2014).

[41] T. Krenke, M. Acet, E. F. Wassermann, X. Moya, L. Mañosa, and A. Planes, Phys. Rev. B **72**, 014412 (2005).

[42] M. Gilleßen, Ph.D. thesis, RWTH Aachen, Germany, 2009.

[43] A. Tavana and L. Makaeilzadeh, AIP Adv. **5**, 117210 (2015).

[44] J. Bai, N. Xu, J. Raulot, Y. D. Zhang, C. Esling, X. Zhao, and L. Luo, J. Appl. Phys. **112**, 114901 (2012).

[45] A. Dannenberg, Ph.D. thesis, Universität Duisburg-Essen, Germany, 2011.

[46] S. R. Barman, A. Chakrabarti, S. Singh, S. Banik, S. Bhardwaj, P. L. Paulose, B. A. Chalke, A. K. Panda, A. Mitra, and A. M. Awasthi, Phys. Rev. B **78**, 134406 (2008).

[47] A. N. Vasil'ev, A. D. Bozhko, V. V. Khovailo, I. E. Dikshtein, V. G. Shavrov, V. D. Buchelnikov, M. Matsumoto, S. Suzuki, T. Takagi, and J. Tani, Phys. Rev. B **59**, 1113 (1999).

[48] G. Bergerhoff and I. D. Brown, in *Crystallographic Databases*, edited by F. H. Allen *et al.* (International Union of Crystallography, Chester, 1987).

[49] A. Belsky, M. Hellenbrandt, V. L. Karen, and P. Luksch, Acta Crystallogr. B **58**, 364 (2002).

[50] M. Pugaczowa-Michalska, J. Magn. Magn. Mater. **320**, 2083 (2008).

[51] M. E. Gruner, P. Entel, I. Opahle, and M. Richter, J. Mater. Sci. **43**, 3825 (2008).

[52] K. Ullakko, J. Huang, C. Kantner, R. O'Handley, and V. Kokorin, Appl. Phys. Lett. **69**, 1966 (1996).

[53] F. Albertini, L. Morellon, P. A. Algarabel, M. R. Ibarra, L. Pareti, Z. Arnold, and G. Calestani, J. Appl. Phys. **89**, 5614 (2001).

[54] T. Sakon, Y. Adachi, and T. Kanomata, Metal **3**, 202 (2013).

[55] R. Tickle and R. D. James, J. Magn. Magn. Mater. **195**, 627 (1999).

[56] S. V. Faleev, Y. Ferrante, J. Jeong, M. G. Samant, B. Jones, and S. S. P. Parkin, Phys. Rev. Mater. **1**, 024402 (2017).

[57] D. Li, A. Smogunov, C. Barreteau, F. Ducastelle, and D. Spanjaard, Phys. Rev. B **88**, 214413 (2013).

[58] J. Enkovaara, A. Ayuela, L. Nordström, and R. M. Nieminen, J. Appl. Phys. **91**, 7798 (2002).

[59] See Supplemental Material at http://link.aps.org/supplemental/10.1103/PhysRevB.98.014411 for the MAE of the local minima ($c/a < 1$), the calculated magnetic moments in comparison to literature values for Ni-based Heusler compounds. In addition, the total energy depending on the c/a ration is provided for the quaternary phases discussed in Sec. IV B 3.

[60] J. H. van Vleck, Phys. Rev. **52**, 1178 (1937).

[61] E. Abata and M. Adsente, Phys. Rev. **140**, A1303 (1965).

[62] I. Galanakis, J. Phys.: Condens. Matter **16**, 3089 (2004).

[63] S. Skaftouros, K. Özdoğan, E. Şaşıoğlu, and I. Galanakis, Phys. Rev. B **87**, 024420 (2013).